Synthesis, characterization and initial biological evaluation of [^{99m}Tc]Tc-tricarbonyl labeled DPA-α-MSH peptide derivatives for potential melanoma imaging

Gao, F.; Sihver, W.; Bergmann, R.; Belter, B.; Bolzati, C.; Salvarese, N.; Steinbach, J.; Pietzsch, J.; Pietzsch, H.-J.;

Originally published:

April 2018

ChemMedChem 13(2018)11, 1146-1158

DOI: https://doi.org/10.1002/cmdc.201800110

Graphics

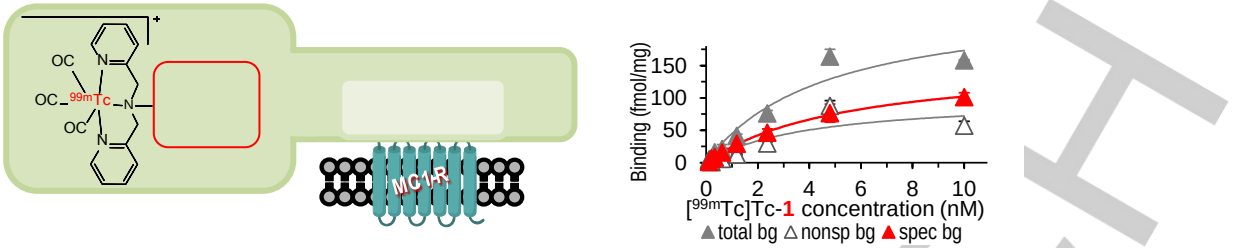

Potential SPECT ligands for imaging melanoma – Using easy ^{99m}Tc-labeling via tricarbonyl, NAPamide conjugates with high affinity to MC1 receptors and good stability in human serum can be prepared in a short time frame and delivered for diagnostic investigations.

FULL PAPER

Synthesis, characterization and initial biological evaluation of [^{99m}Tc]Tc-tricarbonyl labeled DPA-α-MSH peptide derivatives for potential melanoma imaging

Feng Gao,[a] Wiebke Sihver,*[a] Ralf Bergmann,[a] Birgit Belter,[a] Cristina Bolzati,[b] Nicola Salvarese,[b] Jörg Steinbach,[a][c] Jens Pietzsch,[a][c] and Hans-Jürgen Pietzsch[a][c]

[a] Dr. Feng Gao, Dr. Wiebke Sihver, Dr. Ralf Bergmann, Dr. Birgit Belter, Prof. Dr. Jörg Steinbach, Prof. Dr. Jens Pietzsch, Dr. Hans-Jürgen Pietzsch
Institute of Radiopharmaceutical Cancer Research
Helmholtz-Zentrum Dresden-Rossendorf
01328 Dresden,Germany
E-mail: w.sihver@hzdr.de

[b] Dr. Cristina Bolzati, Dr. Nicola Salvarese
Institute of Condensed Matter Chemistry and Technologies for Energy-ICMATE-CNR
35127 Padova, Italy

[c] Prof. Dr. Jörg Steinbach, Prof.Dr. Jens Pietzsch, Dr. Hans-Jürgen Pietzsch
Department of Chemistry and Food Chemistry
School of Science
Technische Universität Dresden
01062 Dresden, Germany

Abstract: α-Melanocyte stimulating hormone (α-MSH) derivatives target the melanocortin-1 receptor (MC1R) specifically and selectively. In this study, the α-MSH derived peptide NAP-NS1 (Nle-Asp-His-D-Phe-Arg-Trp-Gly-NH_2) with and without linkers was conjugated with 5-(bis(pyridin-2-yl)methyl)amino)pentanoic acid (DPA-COOH) and labeled with [^{99m}Tc]Tc-tricarbonyl by two methods. With the one-pot method the labeling was faster than with the two-pots method, however obtaining similarly high yields. Negligible transchelation and high stability in physiological solutions was determined for the [^{99m}Tc]Tc-tricarbonyl-peptide conjugates. Coupling an ethylenglycol (EG)-based linker increased the hydrophilicity. The peptide derivatives displayed high binding affinity in murine B16F10 melanoma cells as well as in human MeWo and TXM13 melanoma cell homogenate. Preliminary in vivo studies with one of the [^{99m}Tc]Tc-tricarbonyl-peptide conjugates showed good stability in blood and both a renal and hepatobiliary excretion. Biodistribution was performed on healthy rats to gain initial insights into the potential relevance of the ^{99m}Tc-labeled peptides for in vivo imaging.

Introduction

Radiolabeled peptides are valuable attractive biological tools for tumor imaging and targeted radionuclide therapy since they can be designed for certain, often overexpressed receptor proteins on tumor cells with favorable pharmacokinetics and specific tumor targeting properties.[1] The melanocortin-1 receptor (MC1R), a G-protein coupled receptor, is overexpressed in melanoma and binds with high affinity the α-melanocyte stimulating hormone (α-MSH).[2] Melanoma, developed from degraded melanocytes, is one of the most aggressive types of skin cancer when metastases are formed. Thus, there is a great need to develop suitable diagnostic tools, e.g. effective tracers for precise detection of melanoma, especially for metastatic melanoma.[3] In recent years different α-MSH derivatives have been developed, conjugated with chelators and radiolabeled for imaging. One of the α-MSH analogs, NAPamide ([Ac-Nle^4,Asp^5,*D*-Phe^7]α-MSH_{4-11}), has been labeled with several radionuclides such as ^{111}In, $^{67/68}$Ga, ^{64}Cu and even ^{44}Sc and showed high affinity to MC1Rs as well as good tumor uptake in tumor bearing mice.[4] However, their potential use for melanoma targeting is limited due to increased kidney accumulation. Furthermore, for better stability against enzymes cyclized[5] α-MSH peptides have been developed. Such radiolabeled derivatives also revealed good tumor uptake, however, with the disadvantage of even more non-specific retention of radioactivity in the kidney.[6]

Currently, there is considerable interest in using ^{99m}Tc-labeled peptides owning favorable chemical and imaging properties for application in SPECT, an imaging technique in common clinical use. Its half life of 6 h gives enough time to prepare ^{99m}Tc-labeled radiopharmaceuticals and perform tumor imaging, but still short enough to keep the radiation exposure short to patients.[7] An indirect labeling approach based on organometallic Tc carbonyl complexes exhibits high stability and high specific activity because of d^6 electron configuration of the Tc(I). The functional species is [[^{99m}Tc]Tc$(CO)_3(H_2O)_3]^+$, which substitutes water molecules with mono-, di- and tridentate ligands.[8] In this regard, tridentate chelators such as (pyridin-2-yl-methyl-amino)-diacetic acid (PADA),[9] functionalized bis(pyridin-2-ylmethyl)amine (DPA)[10] and histidine derivatives[11] are used to form stable complexes and are superior to bidentate chelators where one water molecule remains in the coordination sphere. The synthesis, i.e. the conjugation of the chelator to the peptides is easy, likewise the ^{99m}Tc-labeling. Raposinho et al. studied a [^{99m}Tc]Tc$(CO)_3$-labeled pyrazolyl-α-MSH analog ([Ac-Nle^4,Asp^5,*D*-Phe^7,Lys^{11}(pz-[^{99m}Tc]Tc$(CO)_3$)]α-MSH_{4-11}), which represented high in vitro stability for melanoma targeting. A clear tumor uptake was obtained in murine melanoma-bearing mice. The in vivo specificity of the radiopeptide to MC1R were demonstrated by receptor blocking studies with the potent NDP-MSH. However, blood metabolites appeared already after 1h and both liver and kidney uptake were rather high.[12]

Linkers might act as pharmacological modifier and affect the pharmacokinetic profiles of radiolabeled peptides. The introduction of a linker between a radionuclide chelating agent complex and a peptide can also influence the physicochemical properties. As separator between chelator and peptide a linker is useful to prevent steric effects of the chelator and might change binding properties.[13]

In the present study, for targeting the MC1R the NAPamide NAP-NS1 = Nle-Asp-His-D-Phe-Arg-Trp-Gly-NH_2 was prepared with two different linkers: ε-Ahx (aminohexanoic acid)-β-Ala-linker

(Figure 1a) as well as an ethylene glycol (EG)-based linker (Figure 1b) and compared with NAP-NS1 without linker (Figure 1c). One important aim was to prepare a conjugated peptide in a way that it could easily be labeled with ^{99m}Tc and thus provide a potential applicable radiopharmaceutical. Therefore, functionalized DPA was used as the bifunctional chelator for [^{99m}Tc]Tc-tricarbonyl labeling. An one-pot and a two-pots method for the preparation of the [^{99m}Tc]Tc-DPA-peptide conjugates were compared. The influence of different linkers of the [^{99m}Tc]Tc-tricarbonyl labeled peptides should be investigated with regard to radiochemical and radiopharmacological properties. Advantages and disadvantages of the chelate unit [^{99m}Tc]Tc-tricarbonyl-DPA were discussed. In most of the studies reported in the literature allograft (murine) melanoma models, particularly, using B16F1 or B16F10 cells that exhibit moderate to high MC1R expression,[4b,14] were applied for radiopharmacological characterization. These models only remotely reflect the conditions in human malignant melanoma with comparably lower receptor expression. Of note, regulation of MC1R expression in mouse and human melanoma cells is different.[2] Thus, of particular interest was the study of the novel peptides not only on murine melanoma cells but also on human melanoma cells. Since human melanoma cells often show low MC1R expression in vitro[14,15] respective xenograft models would also be characterized by low receptor expression. In the present study, for want of an adequate human melanoma model, first in vivo biodistribution studies were carried out on healthy rats to gain initial insights into the potential relevance of the ^{99m}Tc-labeled peptides for in vivo imaging and for first dosimetry aspects.

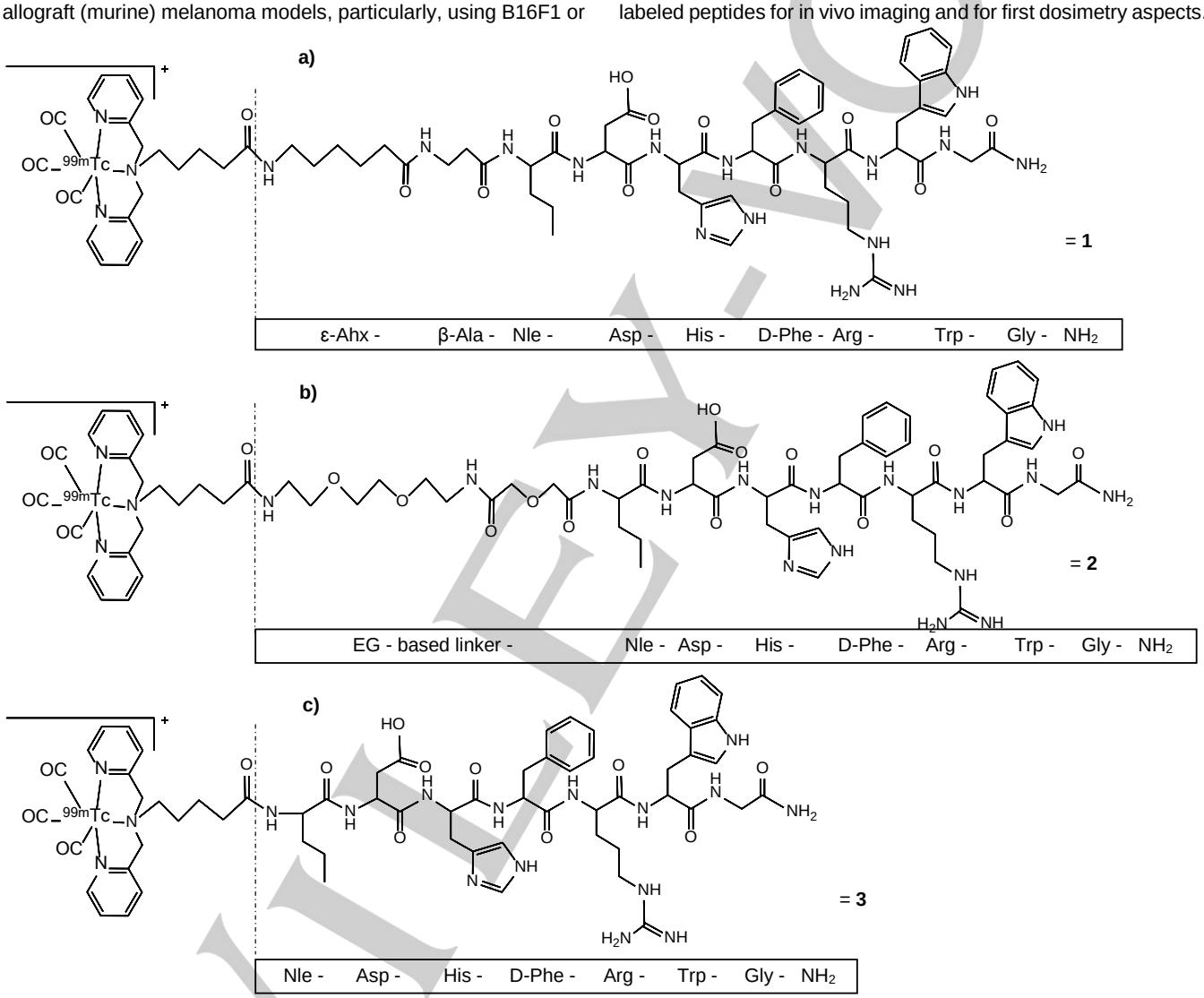

Figure 1. Proposed chemical structures for the ^{99m}Tc-labeled DPA-peptides. **a)** [^{99m}Tc]Tc-**1**; **b)** [^{99m}Tc]Tc-**2**; **c)** [^{99m}Tc]Tc-**3**.

Results and Discussion

Preparation of the NAP-NS1 linker conjugates and coupling with DPA

The EG-based linker was easily coupled to NAP-NS1 with yields of about 33%. The Fmoc-protected ε-Ahx–β-Ala and the EG-based linker were conjugated to NAP-NS1, followed by the deprotection of the Fmoc group with piperidine and purification by semi-preparative HPLC. The identity of the conjugates ε-Ahx-β-Ala-NAP-NS1 and EG-based linker-NAP-NS1 was confirmed by ESI-MS and gathered in Table 1. DPA-conjugated peptides were synthesized from DPA-COOH and the linker-coupled peptides by straightforward bioconjugate techniques within two steps. Firstly, the peptide coupling reagent COMU reacted with DPA-COOH in dry dimethylformamide (DMF) to get the DPA-active ester. Diisopropylamine was used to afford base condition. Secondly, the DPA-active ester was added to the corresponding peptide at a ratio of 1:1 in dry DMF. DPA was easy to couple with the amino

group of the peptide by trans-esterification. After separation with semi-preparative HPLC, the purity of all DPA-conjugated peptides was higher than 99%. The yield of the DPA-peptides with ε-Ahx-β-Ala linker, EG-based linker and without linker was 42%, 38% and 45%, respectively. The peptide conjugates were characterized by MALDI-TOF-MS (Table 1).

Preparation of non-radioactive Re-DPA-peptides

The non-radioactive Re-DPA-peptides (Re-**1**, Re-**2** and Re-**3**) were used as reference compounds and prepared by ligand exchange reaction mixing the complex $(NEt_4)_2[ReBr_3(CO)_3]$[16] and the selected DPA-peptides in absolute ethanol at a ratio of 1:1. After separation by semi-preparative HPLC, the chemical identity of the Re-DPA-peptides was confirmed by MALDI-TOF-MS (Table 1). Yields of Re-DPA-peptides over 55% were obtained.

Labeling of the DPA-peptides with [^{99m}Tc]Tc-tricarbonyl core

The DPA-peptides were labeled with ^{99m}Tc either by a one-pot method or by a two-pots method. It is expected that the chemical structure of the [^{99m}Tc]Tc-tricarbonyl labeled chelate is the same as for the non-radioactive Re-DPA-complex.

Table 1. Summary and identification of the precursors and non-radioactive substances.

Substance	Formula	m/z [M+H]$^+$ calc	m/z [M+H]$^+$ found
EG-based linker-NAP-NS1	$C_{54}H_{78}N_{16}O_{14}$	1176.30	1176.65
1	$C_{70}H_{95}N_{19}O_{12}$	1395.62	1396.23
Re-**1**	$C_{70}H_{95}N_{19}O_{12}Re$	1665.86	1666.39
2	$C_{71}H_{97}N_{19}O_{15}$	1457.65	1457.38
Re-**2**	$C_{71}H_{97}N_{19}O_{15}Re$	1729.91	1727.78
3	$C_{61}H_{79}N_{17}O_{10}$	1211.39	1211.37
Re-**3**	$C_{61}H_{79}N_{17}O_{10}Re$	1483.65	1481.55

For the one-pot method, fresh eluted [^{99m}Tc]TcO_4^-, DPA-conjugated peptide solution and MES buffer (1 M, pH7) were added into a commercial available Isolink kit for $[[^{99m}Tc](CO)_3]^+$ generation.[17] The mixture was heated (95°C, 30 min) obtaining the final ^{99m}Tc-labeled peptides in very high yields (> 95%) of ^{99m}Tc-labeled peptides (Figure 2).

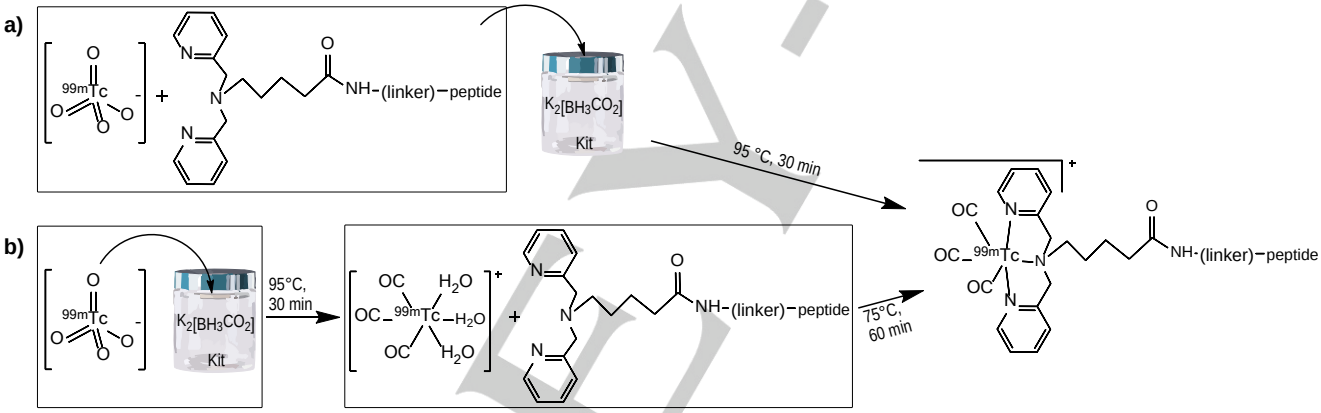

Figure 2. Formation of [^{99m}Tc]Tc-DPA-peptides, **a)** one-pot method, **b)** two-pots method.

Alternatively and for comparative purpose, the [^{99m}Tc]Tc-DPA-peptides were obtained following the standard two-steps (two-pots) procedure[18] in which the first step was required to prepare the $[[^{99m}Tc]Tc(CO)_3(H_2O)_3]^+$ precursor by adding fresh eluted [^{99m}Tc]TcO_4^- to the commercial available Isolink kit (Figure 3). In this step, high temperature (95°C for 30 min) and basic pH (~ 9) are required to generate the $[[^{99m}Tc]Tc(CO)_3(H_2O)_3]^+$ precursor with a high radiochemical yield (> 90%). After the [^{99m}Tc]Tc-tricarbonyl precursor was formed, MES buffer was added to the kit to adjust the pH to around 7. In the second step, the obtained $[[^{99m}Tc]Tc(CO)_3(H_2O)_3]^+$ was mixed with the [^{99m}Tc]Tc-DPA-peptide solutions at 75°C for 60 min to get the ^{99m}Tc-labeled peptides in yields of > 85%.

In both cases the radiochemical yields of the radiolabeled peptides ware comparable, indeed the HPLC analysis of the reaction mixture revealed the existence of a single peak of the respective [^{99m}Tc]Tc-DPA-peptide. With respect to the standard two steps procedure, the one-pot method allows the preparation of the final compounds in nearly physiological pH (7) and the significant shortening of the whole labeling process time. Despite the one-pot method is easy to handle, as expect, high tempera-

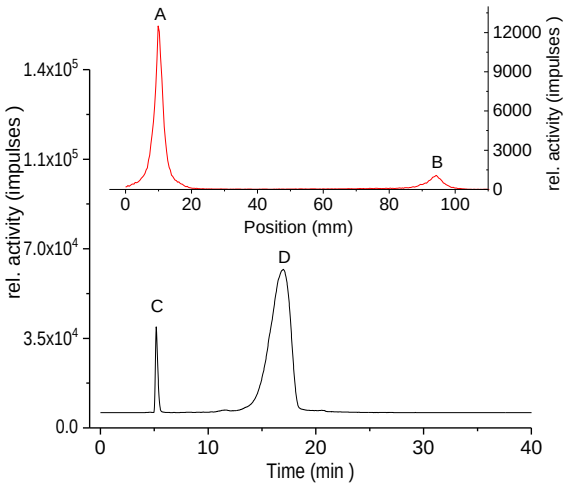

Figure 3. Radio-ITLC (up, red) and radio-HPLC chromatogram (down, black) of the [^{99m}Tc]Tc-tricarbonyl precursor. The peaks A and D are related to the [^{99m}Tc]Tc-tricarbonyl precursor, the peaks B and C are related to pertechnetate.

ture is essential to assure the formation of the [^{99m}Tc]Tc-tricarbonyl core and to complete the labeling process.
Table 2 shows the retention times of the DPA-peptides, the Re-DPA-peptides and the [^{99m}Tc]Tc-DPA-peptides. The [^{99m}Tc]Tc-DPA-peptides could be easily separated from the DPA-peptides since their retention times were shorter than that of the [^{99m}Tc]Tc-DPA-peptides; this enables to get a high molar activity.

Table 2. Radiochemical yields of the ^{99m}Tc-labeled peptides, and retention times of them as well as of the non-labeled peptides obtained by HPLC analysis

Radiolabeled	Radiochemical yields/%*		R_t/min	Starting peptides	R_t/min	Non-radioactive peptides	R_t/min
	One-pot	Two-pots					
[^{99m}Tc]Tc-**1**	97.3 ± 2.1	87.6 ± 1.8	23.1	**1**	19.3	Re-**1**	22.9
[^{99m}Tc]Tc-**2**	96.1 ± 0.9	86.4 ± 1.1	23.3	**2**	20.0	Re-**2**	23.0
[^{99m}Tc]Tc-**3**	95.8 ± 1.3	89.3 ± 0.7	24.2	**3**	19.4	Re-**3**	24.0

*Two-pot yields cannot be higher than 90%, since the yield of the intermediate complex [[^{99m}Tc]Tc$(CO)_3(H_2O)_3$]$^+$ was about 91%.

After radiolabeling, the chemical identity of the [^{99m}Tc]Tc-DPA-peptides were confirmed by HPLC comparison with the corresponding Re-analogs characterized by MALDI-TOF MS analysis. [^{99m}Tc]Tc-DPA-peptides displayed the same retention times as the Re-DPA-peptides (Figure 4).

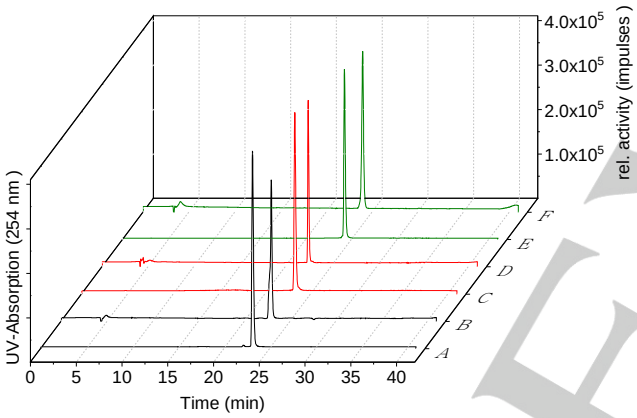

Figure 4. Radio-chromatograms of ^{99m}Tc-labeled DPA-peptides and UV-chromatograms of corresponding non-radioactive Re-DPA-peptides. All HPLC runs are performed under the same conditions. **A**: Radio-chromatogram of [^{99m}Tc]Tc-**1**; **B**: UV-chromatogram of Re-**1**; **C**: Radio-chromatogram of [^{99m}Tc]Tc-**2**; **D**: UV-chromatogram of Re-**2**; **E**: Radio-chromatogram of [^{99m}Tc]Tc-**3**; **F**: UV-chromatogram of Re-**3**.

The generation of the [^{99m}Tc]Tc-tricarbonyl core needs high pH and high temperature, while to prepare [^{99m}Tc]Tc-tricarbonyl-complex could be performed under mild conditions. This would be preferred for labeling substances that could not tolerate high pH and high temperature, for example antibodies or proteins.[19]

Stability

For in vitro stability studies, [^{99m}Tc]Tc-DPA-peptides were purified by HPLC, neutralized with $NaHCO_3$ and concentrated with a gentle argon stream prior in solutions of phosphate buffered saline (PBS), cysteine, histidine or in serum.[18a] A rapid method was developed for concentration and acid removal in order to facilitate the preparation of new radiotracers for in vivo evaluations.

Stability of [^{99m}Tc]Tc-**1**, [^{99m}Tc]Tc-**2** or [^{99m}Tc]Tc-**3** were determined with HPLC monitoring the variation of the radiochemical purity of the compounds after incubation in PBS and human serum for 1h and 24h. The compounds remained stable in the reaction solutions (> 97% after 24 h) (Table 3). In previous studies, on the corresponding ^{64}Cu-labeled NOTA- and [^{99m}Tc]Tc(N)(PNP3)]-labeled NAP-NS-peptides also showed high stability in PBS and serum, with over 97% intact complex in the supernatant.[4e,20]
The transchelation challenge for the [^{99m}Tc]Tc-DPA-peptides with an excess of free histidine (1 mM, 10 mM) and cysteine (1 mM, 10 mM) also showed high stability of the radiolabeled peptides; only negligible variations of radiochemical purity was found after 24 h of incubation in the challenge solutions at 37°C (Table 3). Under these conditions no radiolysis was observed. This occurrence has been previously reported by Radford et al.[18a] for another class of [^{99m}Tc]Tc-DPA labeled peptides for whose the addition of a radioprotective agent such as gentisic acid and an adjustment of the pH to 7.4 was necessary to improve their stability.[21] High challenge stability confirmed that the coordination between [^{99m}Tc]Tc-tricarbonyl and DPA apparently is sufficient for in vivo use as it has been described earlier.[10b,22]

Table 3. Stability and log $D_{o/w}$ values for the [^{99m}Tc]Tc-DPA-peptides

	[^{99m}Tc]Tc-**1**		[^{99m}Tc]Tc-**2**		[^{99m}Tc]Tc-**3**	
Stability (%)	1 h	24 h	1 h	24 h	1 h	24 h
PBS	>99.5	>97.0	>99.5	>98.0	>99.6	>98.0
Human serum	>99.5	>97.0	>99.5	>99.0	>98.0	>98.0
1 mM cysteine	>99.5	>97.0	>99.5	>99.0	>99.5	>98.0
10 mM cysteine	>99.5	>97.0	>99.5	>98.0	>99.0	>99.0
1 mM histidine	>99.0	>97.0	>99.5	>98.0	>99.5	>98.5
10 mM histidine	>99.5	>97.0	>99.5	>98.0	>99.0	>98.5
log $D_{o/w}$*	-0.43 ± 0.01		-0.92 ± 0.02		-0.05 ± 0.01	

*Mean values are reported ± SD; n = 3.

Binding to the serum proteins and in vitro metabolism of the [^{99m}Tc]Tc-DPA-peptides were assessed by incubating the purified compounds in human serum at 37 °C for 1 and 24 h. Low binding to the serum proteins (less than 15%) was detected for [^{99m}Tc]Tc-**1**, [^{99m}Tc]Tc-**2** and [^{99m}Tc]Tc-**3** when precipitated by ethanol. HPLC analysis of the radioactivity left in the supernatant displayed minimal decomposition of all the [^{99m}Tc]Tc-DPA-peptides both at

1 and 24 h of incubation (Table 3). Notably, the insertion of linkers between the chelator and the amino acid sequence did not affect the stability of our compounds. These data are in perfect agreement with our previous studies, on the corresponding [^{64}Cu][Cu]-NOTA- and [^{99m}Tc][Tc(N)(PNP3)]-labeled NAP-NS1-peptides.[4e,20]

Determination of octanol/water distribution coefficient

The distribution coefficients log $D_{o/w}$ (Table 3) of the [^{99m}Tc]Tc-DPA-peptides, determined by the "shake flask" method, suggested good hydrophilicity for the radiolabeled peptides. [^{99m}Tc]Tc-**3** displayed less hydrophilic character than [^{99m}Tc]Tc-**1** and [^{99m}Tc]Tc-**2**, implying that the linkers increased the hydrophilicity. Still, the hydrophilicity was somewhat lower than for [^{64}Cu]Cu-NOTA- and [^{99m}Tc][Tc(N)(PNP3)]-NAPamide analogs in earlier studies,[4e,20] likely due to the lipophilic tendency of the carbonyl groups. Moreover, cyclic α-MSH analogs showed higher hydrophilicity than linear peptides.[4e,20,23] However, in the study from Raposinho et al.[24] the cyclic ^{99m}Tc-labeled α-MSH analog was moderately hydrophobic in comparison to the hydrophilic linear peptide. It is worth to note that the [^{99m}Tc]Tc-DPA-peptides showed a tendency to stick on the wall of vials or injection glass syringes. To avoid this adsorption phenomenon, radiolabeled peptides were dissolved in MES buffer (pH 6.2) containing 10% ethanol after evaporation of the elution solvent.

Cell binding assays

The receptor-binding affinities of NAP-NS1, **1**, **2**, **3**, Re-**1**, Re-**2**, Re-**3** and standard compound NDP-MSH were evaluated by competition binding assays against [^{125}I]I-NDP-MSH in B16F10 and MeWo cell homogenate. Applying the K_d values from [^{125}I]I-NDP-MSH of 0.19 ± 0.01 nM and 0.23 ± 0.03 nM in B16F10 and MeWo homogenate (determined in-house), respectively, into the Cheng-Prusoff equation, the K_i values were determined (Table 4). In B16F10 cells all the peptide complexes showed high binding affinities with values in the low nanomolar range (Figure 5). The affinity of the standard compound NDP-MSH with a K_i value of 0.01 ± 0.001 nM was considerably higher than that of the other new conjugated peptides. Coupling the linker and coordinating the metal rhenium to the peptide did cause only slight loss of binding affinity. Different linkers do not have obvious influence on the binding affinity of the peptide complexes. In MeWo cells, ε-Ahx–β-Ala-NAP-NS1, **1** and Re-**1** also showed high binding affinities with comparable K_i values, but slightly worse than the standard compound NDP-MSH (K_i 0.7 nM).The K_i values of **1**, **2**, **3**, Re-**1**, Re-**2**, Re-**3** are even well comparable with those of the NOTA-peptides and ^{nat}Cu-NOTA-peptides.[4e] Substitution of the chelator NOTA to DPA influenced the binding affinity of the peptides negligible. Binding affinity of α-MSH derivatives from other research groups were mainly presented as IC_{50}. This affords a tendency about high or low affinity; however it is not directly comparable with values from the present study.

The murine standard cell line B16F10 expressing MC1R was used to investigate binding in comparison with data from other studies. However, the present study was aimed to characterize the binding in MC1R expressing human melanoma cells, MeWo and TXM13, in order to identify an appropriate mouse model for further investigations. Only the MC1R subtype from the MCR family (MC1R to MC5R) has been found in melanocytes and is expressed around 10-20 times higher in melanoma tissues and cultured melanoma cells in comparison to receptor expression in healthy skin tissue.[25] Even though the standard [^{125}I]NDP-MSH derived from α-MSH could bind to MC1, MC3, MC4 and MC5 receptors without selectivity,[26] it is worthwhile to develop appropriate MC1R peptides due to its overexpression in melanomas.

[^{125}I]NDP-MSH expressed high binding affinity in the three cell lines B16F10, MeWo and TXM13 with K_d values in reasonably agreement with earlier data.[14,26b,27] However, [^{125}I]NDP-MSH had a tendency to exhibit slightly lower affinity to MeWo cells compared to murine B16F10 cells in this study, likely due to differences between murine and human MC1Rs as they share only a homology of about 70%.[28] Compared with the other NAPamides investigated, unlabeled NDP-MSH had the highest affinity not only in the murine cell line as also found by Chen et al,[29] but also in human cells. Thus, the binding affinity of **1** and Re-**1** was also in the low nanomolar range in human MeWo cells. A slight decrease of binding affinity was observed after coupling the ε-Ahx-β-Ala linker and the EG-based linker as well as DPA to NAP-NS1.

Table 4. K_i values of three native peptides, **1**, **2**, **3**, Re-**1**, Re-**2**, Re-**3** and NDP-MSH on B16F10 and MeWo cell homogenate.*

	K_i (nM)	DPA	K_i (nM)	Re-DPA	K_i (nM)
B16F10					
ε-Ahx–β-Ala NAP-NS1	0.5 ± 0.1	**1**	1.5 ± 0.1	Re-**1**	3.0 ± 0.8
EG-based NAP-NS1	0.7 ± 0.2	**2**	1.3 ± 0.2	Re-**2**	1.8 ± 0.3
NAP-NS1	0.5 ± 0.1	**3**	1.8 ± 0.3	Re-**3**	1.2 ± 0.1
NDP-MSH	0.01 ± 0.001				
MeWo					
ε-Ahx–β-Ala NAP-NS1	1.2 ± 0.1	**1**	1.1 ± 0.1	Re-**1**	2.8 ± 0.3
NDP-MSH	0.7 ± 0.1				

***Mean values are reported ± SD; n = 3.

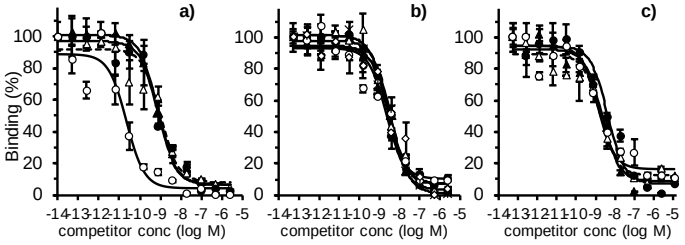

Figure 5. Representative competition curves of ε-Ahx-β-Ala-NAP-NS1, EG-based linker-NAP-NS1 and NAP-NS1 as well as **1**, **2**, **3** and Re-**1**, Re-**2**, Re-**3**, and NDP-MSH versus [^{125}I]I-NDP-MSH binding; **a)** on B16F10, ▲ NAP-NS1, △ NAP-NS1(β-Ala), ● NAP-NS1(EG-based), ○ NDP-MSH; **b)** on B16F10, ▲ **1**, △**2**, ●**3**, ○ Re-**1**, ◇ Re-**2**, ∗ Re-**3**; **c)** on MeWo cells, ▲ NAP-NS1(β-Ala), △**1**, ● Re-**1**, ○ NDP-MSH. Each data point arises from 3 samples. The assays were performed in triplicate.

NAPamide has been studied before,[4a,30] showed there also high affinity to the MC1R and some loss of affinity after conjugation with a chelator. Interestingly, after insertion of Re to DPA-peptide without linker (**3**), the affinity was not changed. After insertion of ^{nat}Cu to DOTA-NAPamide Cheng et al.[4b] also observed some affinity decrease.The MC1R affinities of the linear peptide conjugates **1**, **2**, **3** and Re-**1**, Re-**2**, Re-**3** were high in comparison to the cyclic peptide NAP-NS2 investigated before (K_i > 10 nM).[4e]

However, other cyclized α-MSH derivatives with rhenium in the cycle had affinities in the subnanomolar and low nanomolar range;[6c,31] moreover, the affinity of DOTA-glycine-cycled MSH[32] as well as β-Ala-Nle-cyclic α-MSH derivatives[33] based on melanotan II was in the same range as **1**, **2**, **3** and Re-**1**, Re-**2**, Re-**3**. Differences in binding affinity to the MC1R between linear and cyclic peptides occur due to varying amino acid sequences, steric effects, polarity, flexibility and charge effects.

Saturation. Typical saturation graphs were obtained using the [^{99m}Tc]Tc-tricarbonyl labeled DPA-peptides in homogenate of B16F10, MeWo and TXM13 cells and compared with the results of the standard peptide [^{125}I]I-NDP-MSH. The K_d and B_{max} values are presented in Table 5. The [^{99m}Tc]Tc-DPA-peptides showed high affinity with K_d values in the low nanomolar range in the three melanoma cell lines. The highest affinity presented the standard peptide [^{125}I]I-NDP-MSH. The B_{max} values were lower in the human melanoma cells MeWo and TXM13. The nonspecific binding was < 20% at concentrations of about K_d for all [^{99m}Tc]Tc-DPA-conjugates and [^{125}I]I-NDP-MSH on B16F10 homogenate, as well as for [^{99m}Tc]Tc-**1** on MeWo cell homogenate. The nonspecific binding for [^{99m}Tc]Tc-**1** on TXM13 cells, as well as for [^{125}I]I-NDP-MSH on MeWo and TXM13 cells was 30-45% at concentration of K_d. Furthermore, adjacent assays with [^{99m}Tc]Tc-DPA-peptides and [^{125}I]I-NDP-MSH using the MC1R negative cell line HEK-293 revealed no specific binding. The affinities of [^{99m}Tc]Tc-DPA-peptides in the nanomolar range are sufficient for imaging. The B_{max} values of [^{99m}Tc]Tc-DPA-peptides on B16F10 cells were consistent, implying that the linkers do not have steric influence on peptides, retaining the same binding capacity. In comparison to the ^{64}Cu-labeled NOTA-peptides, the insertion of linkers changed the steric structure of the peptide, resulting in a decreased binding capacity to MC1Rs.[4e,20]

The human metastatic cell line MeWo has been shown to clearly express MC1Rs[34] and was applied as orthotopic tumor mouse model.[35] However, the amount of receptors per cell at the MeWo cell surface is much lower than those in murine B16F10. It is reported that around 20,000 binding sites per cell were found in murine B16F10 cells.[4b] The human melanoma cell line TXM13 has been reported to express about 5700 MC1Rs per cell[15] that is a rather high amount for a human melanoma cell line.[14] The affinity of [^{125}I]I-NDP-MSH was in the same magnitude for the murine B16F10 and for human cells, for latter however much lower specific binding sites. The K_d values of the [^{99m}Tc]Tc-DPA-peptides were also in the same range for murine and human cells; the B_{max} values was several times higher in the murine cell line, however it could be shown that TXM13 cells express some MC1Rs more than MeWo cells. The comparison of the K_d values of the [^{99m}Tc]Tc-DPA-peptides and [^{64}Cu]Cu-NOTA-peptides on B16F10 and MeWo cells suggested similar binding affinity to the MC1Rs.[4e,20] However, [^{99m}Tc]Tc-DPA-peptides showed higher B_{max} than [^{64}Cu]Cu-NOTA-peptides and [^{125}I]I-NDP-MSH in B16F10 as well as in human cells, demonstrating more specific binding capacity. This might be caused due to the fact that the chelating units [^{99m}Tc]Tc-tricarbonyl-DPA has a positive charge whereas the chelating unit [^{64}Cu]Cu-NOTA is negative and [^{125}I]Tyr in [^{125}I]I-NDP-MSH neutral. As the conserved sequence of the peptide (His-D-Phe-Arg-Trp) is responsible for the specific binding, histidine and arginine contribute considerably since they function as proton acceptor that is reinforcing the binding with the chelating unit [^{99m}Tc]Tc-tricarbonyl-DPA. It has been shown that especially Asp^{119} at the extracellular end of the TM3 together with Cys^{271} from the extracellular loop 3 (both conserved) of the MC1R are responsible for agonist binding.[36] Thus, it might be that the negative charges of Asp^{119} and Asp^{115} attract more α-MSH peptide molecules together with His-D-Phe-Arg-Trp and the positively charged chelating unit. This might explain changes in B_{max} compared to α-MSH peptides without chelating units.

Table 5. Binding parameters of [^{99m}Tc]Tc-DPA-peptides on homogenate of B16F10, MeWo and TXM13 cells.

Cell line	B16F10 cells		MeWo cells		TXM13 cells	
Stability (%)	K_d (nM)	B_{max} (fmol/mg)	K_d (nM)	B_{max} (fmol/mg)	K_d (nM)	B_{max} (fmol/mg)
[^{99m}Tc]Tc-**1**	6.0 ± 0.5	404 ± 46	4.5 ± 0.8	50 ± 6	5.4 ± 0.1	170 ± 12
[^{99m}Tc]Tc-**2**	6.8 ± 1.6	428 ± 18	3.5 ± 0.6	118 ± 4	4.8 ± 0.5	192 ± 18
[^{99m}Tc]Tc-**3**	2.6 ± 0.4	457 ± 56	4.5 ± 0.8	93 ± 12	3.7 ± 1.2	164 ± 9
[^{125}I]I-NDP-MSH	0.2 ± 0.01	37 ± 9	0.2 ± 0.03	1.4 ± 0.1	0.3 ± 0.1	8.0 ± 1.6

Determined data are mean ± SEM of 3 assays.

In vivo studies of [^{99m}Tc]Tc-1

In vitro characterization of the synthesized radiopeptides is not sufficient for estimating their potential for further use, hence it is necessary to investigate the accumulation of these peptides and their metabolites in excretion organs as liver and kidney. Thus, initial attempts in male Wistar rats have been performed. Based on the good in vitro stability and binding properties the in vivo studies were performed with [^{99m}Tc]Tc-**1**.

Formation of metabolites in healthy rats. In vivo metabolite analyses were performed by monitoring the stability of [^{99m}Tc]Tc-**1** and accordingly the composition of metabolites in blood and urine of healthy rats. [^{99m}Tc]Tc-**1** shows high stability in blood, HPLC profile of the blood plasma collected at 1 h p.i. clearly show the absence of metabolites. However, in urine the main radioactive peak appeared to be a metabolite (Figure 6). For ^{64}Cu-labeled NOTA-peptide, a negligible metabolite was found in blood plasma at 2 h p.i., and to a small extent in urine.[4e] But in the present study, the metabolite represents the main peak in the urine. The chelating unit [^{64}Cu]Cu-NOTA is negatively charged, while the charge of [^{99m}Tc]Tc-tricarbonyl-DPA is positive. The stability for the important sequence of the developed MSH peptide has been improved by replacing the L-Phe with the non-natural D-Phe.[37] Furthermore, the in vivo stability of peptides can be improved with chelate and linker units, amidation of the C-terminus. These aspects have been so far successfully considered for the peptides presented in this study. An interesting approach would be the formation of dimers, tetramers or heterodimers for increasing the peptide stability.[5b] While passing the kidney, the positively charged [^{99m}Tc]Tc-tricarbonyl-DPA interacts with the molecules of the kidney surface and supposably forms the metabolite, excreted into the urine. The influence of a charge on uptake in the kidney has been referred earlier for radiolabeled peptides.[38] The interaction between positively charged peptide conjugates and negatively charged surface of the proximal tubular cells was increasing the renal uptake.[39] This might in turn increase the radiation nephrotoxicity; hence, it is considered in general that the kidney accumulation is a dose-

limiting factor. Negatively charged MSH peptides contribute to a decreased kidney retention.[40] Thus, to reduce the kidney uptake and retention time neutral of negatively charged peptides might be preferable that could be e.g. influenced by the chelate unit.

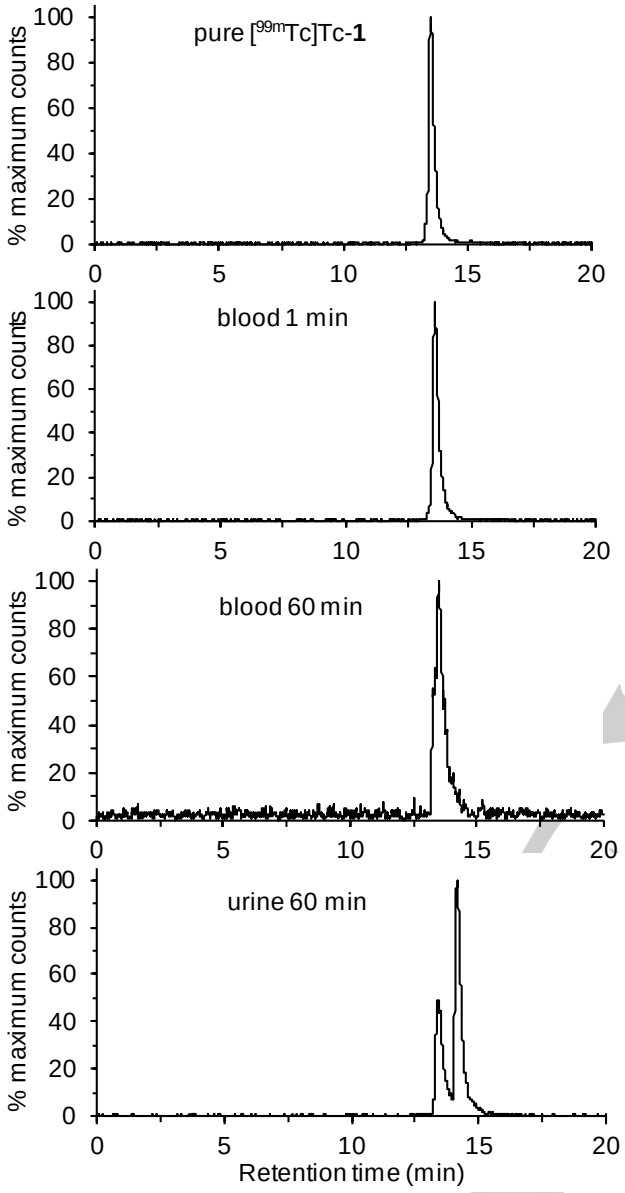

Figure 6. Radio-HPLC chromatograms of blood and urine samples at 1 h p.i. of [^{99m}Tc]Tc-**1** compared to pure [^{99m}Tc]Tc-**1** injection solution. Analysis was performed on a Zorbax C18 300SB (250 × 9.4 mm; 4 µm) column with an eluent system: A (H_2O + 0.1% TFA) and B (CH_3CN + 0.1% TFA); 0 - 30 min 90% - 10% solvent A; flow rate 3 mL/min.

Activity distribution in animal blood. Activity distribution was investigated in rat blood by measuring the activity in blood plasma and blood cells. Moreover, the activity in plasma supernatant and plasma protein pellet were also tested. Activity distribution shows that over 88% of activity was found in plasma; less than 5% of activity was bound to plasma protein pellets (Figure 7). This result is in agreement with the low protein binding of [^{99m}Tc]Tc-**1** in human serum.

In vivo biodistribution studies. Biodistribution studies were performed in male Wistar rats at time points of 5 min and 60 min after intravenous injection of [^{99m}Tc]Tc-**1**, in order to have a first

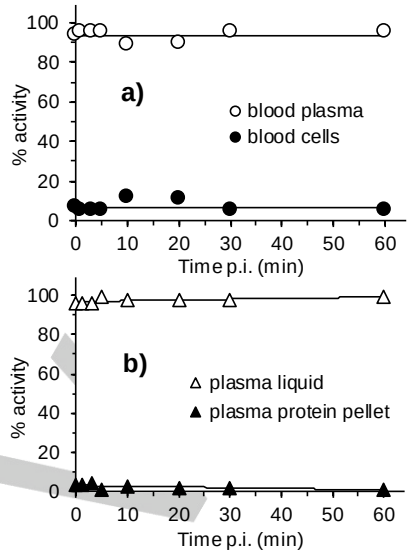

Figure 7. Activity distribution in **a)** rat blood plasma and blood cells as well as in **b)** plasma liquid and plasma protein pellet. Data are representative from one in vivo experiment.

insight into its potential relevance as a radiotracer for in vivo imaging. The biodistribution data of [^{99m}Tc]Tc-**1** are presented in Table 6. The formation of [^{99m}Tc]TcO_4^-, which is readily taken up by the stomach, was not supported by the data, as this organ had low uptake at 5 min that did not increase during 60 min. At 5 min after injection high uptake values were obtained for kidney, liver and intestine, moderately high for lung (Table 6, Figure 8a). The other organs show lower uptake. At 60 min after injection, the uptake in the organs decreased, except for the uptake in the intestine. Since the uptake in the critical radiosensitive organs (kidney, liver and lung) decreased considerably an organ distribution of [^{99m}Tc]Tc-**1** at later time points was not performed in this preliminary trial. At 5 min p.i., the summation of uptake from kidney and urine is lower compared to uptake of liver and intestine. At 60 min p.i., the activity in kidney and urine is higher than in liver and intestine, indicating the elimination via both hepatobiliary and renal route (Figure 8b), presumably due to the lipophilic character of [^{99m}Tc]Tc-tricarbonyl moiety. In the log $D_{o/w}$ study was found that [^{99m}Tc]Tc-**1** was more lipophilic than its counterpart ^{64}Cu-labeled NOTA-ε-Ahx-β-Ala-NAP-NS1 (log $D_{o/w}$ 2.3)[4e] and [^{99m}Tc][Tc(N)(PNP3)]-labeled NAP-NS1-peptide (log $D_{o/w}$ -1.46)[20] changing the elimination route. In the present study, an activity reduction of about 80% was observed both in kidney and liver after 60 min p.i. As already pointed out, the kidney uptake has to be concerned seriously. After filtration by the glomerulus and reabsorption by the tubular cells, small proteins and peptides will be delivered to renal lysosomes and metabolized after hydrolyzation.[41] The final radioactive metabolites do not excrete quickly,[40] though co-injection of L-lysine could significantly reduce the nonspecific kidney accumulation after administration of radiolabeled α-MSH derivatives.[4a,29,30,42] 3.0 ± 1.7% ID/g was obtained for the kidney at 60 min p.i. for [^{99m}Tc]Tc-**1**, similar to the kidney uptake for the corresponding [^{99m}Tc][Tc(N)(PNP3)(NAP-NS1]$^+$ compound (3.40 ± 0.1 ID/g) and for ^{64}Cu-labeled NOTA-

peptide (2.0 ± 1.7% ID/g) 60 min after injection of radiotracer,[4e,20] but it was much lower than that of [^{64}Cu]Cu-DOTA-NAPamide (~ 12% ID/g).[4b] However, the uptake of [^{99m}Tc]Tc-**1** in the liver at 60 min p.i. (4.6 ± 0.5% ID/g) was higher than ^{64}Cu-labeled NOTA-NAP-NS1 uptake (0.8 ± 0.1% ID/g) investigated before, likely due to the higher lipophilicity of [^{99m}Tc]Tc-**1**. Differences in the studies themselves as well as in the chelate units with and without linkers and charges of radioconjugates as well as the use of different animal models make direct comparison difficult.

Table 6. Biodistribution data after injection of 0.3 ± 0.03 MBq of [^{99m}Tc]Tc-**1** (500 µL) in male Wistar rats.

Organ	5 min p.i.	60 min p.i.
Brain	0.04 ± 0.01	0.01 ± 0.00
Pancreas	0.48 ± 0.05	0.36 ± 0.19
Spleen	0.99 ± 0.46	0.43 ± 0.13
Adrenals	0.81 ± 0.11	0.23 ± 0.05
Kidneys	15.41 ± 1.26	2.69 ± 0.34
Heart	0.81 ± 0.11	0.44 ± 0.04
Lung	2.01 ± 0.20	0.68 ± 0.06
Thymus	0.68 ± 0.18	0.20 ± 0.06
Thyroid*	0.06 ± 0.02	0.02 ± 0.00
Liver	7.93 ± 0.47	1.20 ± 0.12
Femur	0.44 ± 0.04	0.15 ± 0.01
Intestine*	6.27 ± 1.25	31.86 ± 1.82
Stomach*	0.71 ± 0.11	0.52 ± 0.25
Blood	0.83 ± 0.01	0.18 ± 0.13
Hair / Skin	0.89 ± 0.04	0.28 ± 0.04
Muscle	0.25 ± 0.02	0.16 ± 0.14
Testes	0.16 ± 0.01	0.15 ± 0.08

Data are expressed as standard uptake value (SUV = ratio of measured radioactivity per tissue weight to injected radioactivity per rat body weight) and presented as mean of 4 rats from each group ± SD; *for these organs data are expressed as %ID/g tissue.

In one study, DPA was used as ^{99m}Tc chelating unit with a triazol linker and a cysteine residue in the α-MSH peptide. In this formation, conjugates show a rather different biodistribution than in present study, namely higher uptake in liver and kidney 1h p.i. and much slower decrease; but unfortunately no metabolite results were provided.[43] Thus, the type of DPA-linker-MC1R-conjugates from present study seems to be a promising alternative for ongoing studies.

Conclusions

In this study, novel 99mTc-labeled α-MSH derivatives were prepared and evaluated for the potential use as a radiotracer for diagnosis of melanoma. The DPA ligand was conjugated to α-MSH derivatives with and without linker, and coordinated by

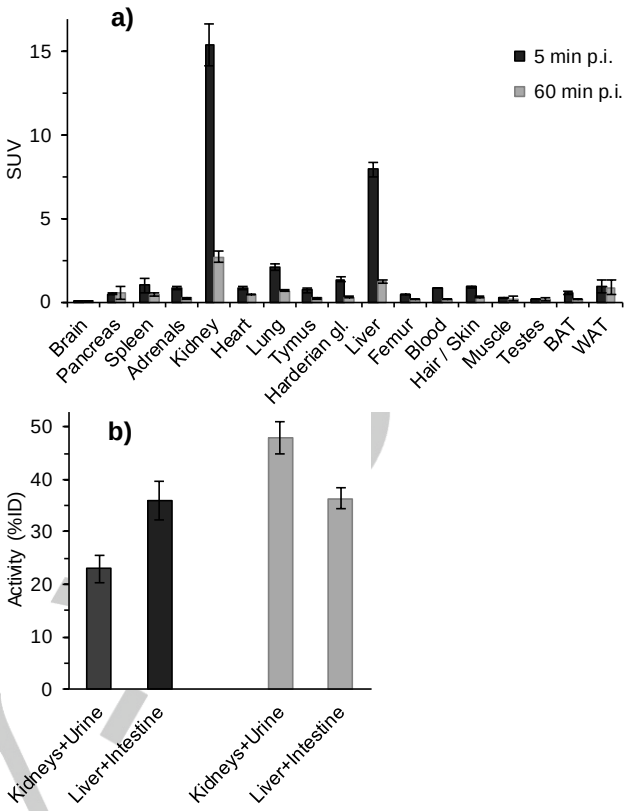

Figure 8. a) Biodistribution after injection of 0.3 ± 0.03 MBq of [^{99m}Tc]Tc-1 (500 µL) in desflurane-anesthetized Wistar rats, 5 min p.i. (black) and 60 min p.i. (gray). Data are expressed in mean SUV ± SD (n = 4), (BAT = brown adipose tissue, WAT = white adipose tissue); **b)** accumulation of [^{99m}Tc]Tc-1 in kidney and urine together as well as in liver and intestine together, at 5 min p.i. (black) and 60 min p.i. (gray), respectively.

[99mTc]Tc-tricarbonyl moiety. The non-radioactive Re-DPA-peptides were used to demonstrate the analogous labeling in the ^{99m}Tc product and for comparison purposes. Exceptional labeling yields and radiochemical purities were achieved for [^{99m}Tc]Tc-DPA-peptides whereat a one-pot method yielded in the final compounds after considerably shortened labeling process time. Coupling the linker to the peptide had negligible influence on pharmacological behaviour in vitro. In vitro stability studies indicated excellent chelation of [^{99m}Tc]Tc-tricarbonyl moiety by DPA-peptide and high stability against enzymes. The peptide conjugates exhibited high binding affinities on murine B16F10 cells as well as on human MeWo and TXM13 cells. Initial in vivo evaluation resulted in one main metabolite found in rat urine 1 h after injection of [^{99m}Tc]Tc-**1**. In rat blood, low protein binding was measured. Elimination of [^{99m}Tc]Tc-**1** via hepatobiliary route and renal route attributed to the lipophilic nature of the [^{99m}Tc]Tc-tricarbonyl moiety. Definitely, [^{99m}Tc]Tc-**1** should be used for further pharmacokinetic studies, however, possibly on human melanoma-bearing mice. Such respective xenograft models would show lower MC1R expression than murine melanoma models. Here, as a model limitation, the inadequate crosstalk, e.g. between mouse hormonal regulation and xenotransplanted tumor cells has to be considered.

Experimental Section

Chemicals and reagents

Na[^{99m}Tc]TcO_4 was eluted from a Mo-99/Tc-99m generator (Covidien, The Netherlands). Two linear peptides NAP-NS1 and ε-Ahx-β-Ala-NAP-NS1 were custom made by GL Biochem, Shanghai, Ltd. The EG-based linker[44] was coupled with NAP-NS1, and the chelator DPA-COOH was synthesized in house. (Nle^4, $D\text{-}Phe^7$)-α-MSH (NDP-MSH) was purchased from Bachem AG, Switzerland. The tricarbonyl labeling agent Isolink kits were provided by Mallinckrodt Medical B.V., Netherland. [^{125}I]I-NDP-MSH was obtained from Biotrend Chemikalien GmbH, Germany. All other chemical and biological reagents were purchased from Sigma Aldrich, USA, and Biochrom AG, Germany, respectively.

Instruments

Semi-preparative high-performance liquid chromatography (HPLC) was used to purify and analyze the conjugates as well as to evaluate the radiochemical yield and the stability as variation of the radiochemical purity of the radiolabeled compounds. Analyses were carried out on a chromatography system equipped with an UV detector (Perkin Elmer UV/VIS LC290) and a radioisotope detector (Ramona, Raytest GmbH, Straubenhardt, Germany) using a reverse phase Zorbax C18 column with an inner diameter of 8 mm. The mobile phase was solvent A: H_2O with 0.1% (v/v) TFA and solvent B: CH_3CN with 0.1% (v/v) TFA; gradient was 95% - 50% solvent A in 30 min and the flow rate was 3 mL/min; (λ = 254 nm).

Electrospray ionization-mass spectrometry (ESI-MS) was carried out with a mass spectrometer (micromass tandem quadrupole mass spectrometer, Waters Corporation, USA). The matrix-assisted laser desorption/ionization time of flight mass spectrometry (MALDI-TOF-MS) mass spectra were measured on a Daltonic Autoflex II TOF/TOF (Bruker Daltonik). Radioactive samples were counted using a gamma counter (1480 WIZARD 3" automatic, PerkinElmer, Inc., USA).

Preparation of EG-based linker-NAP-NS1

Fmoc-EG-based linker[44] (1.46 mg, 3 µmol) and coupling reagent COMU (1.28 mg, 3 µmol) were dissolved in dry DMF (500 µL) with *N*,*N*-diisopropylethylamine (5.2 µL, 30 umol). The mixture was shaken for 15 min at 23°C. Then, NAP-NS1 (12.79 mg, 3 µmol) dissolved in dry DMF (500 µL) was added into the mixture. All was shaken overnight at 23°C. Piperidine (2 mL) and dry DMF (1 mL) was added into the reaction mixture that was then kept in shaking stage for 1 h at 40°C. Thereafter, the mixture was evaporated by a rotary evaporator. The final crude product was dissolved in H_2O (2 mL) and purified with semi-preparative HPLC. The purified EG-based linker-NAP-NS1 was characterized by ESI-MS and MALDI-TOF-MS.

Preparation of the DPA-peptide conjugates

DPA-COOH (0.99 mg, 3.3 µmol) and COMU (1.29 mg, 3.0 µmol) were dissolved in DMF (500 µL) with *N*,*N*-diisopropylethylamine (5.8 µL, 33 µmol) and the mixture was incubated for 15 min at 23°C. Then, either ε-Ahx-β-Ala-NAP-NS1, EG-based linker-NAP-NS1 or NAP-NS1 (each 3.0 µmol), dissolved in dry DMF (500 µL) was added into the mixture and shaken overnight at 23°C. The next day, water (200 µL) with TFA (0.1%) was added into the mixture to stop the reaction. The mixture was separated by semi-preparative HPLC and the purified DPA-peptides DPA-ε-Ahx-β-Ala-NAP-NS1 (**1**), DPA-EG-based linker-NAP-NS1 (**2**) and DPA-NAP-NS1 (**3**) were confirmed by ESI-MS and MALDI-TOF-MS.

Preparation of non-radioactive rhenium-DPA-peptide complexes

$(NEt_4)_2[ReBr_3(CO)_3]$ was synthesized according to literature.[**Error! Bookmark not defined.**] $(NEt_4)_2[ReBr_3(CO)_3]$ (5 µmol) in absolute ethanol (500 µL) was added into DPA-conjugated peptide (5 µmol) in absolute ethanol (500 µL). The mixture shook for 90 min at 60°C. Afterwards, Re-DPA-peptides conjugates Re-**1**, Re-**2** and Re-**3** were separated from $(NEt_4)_2[ReBr_3(CO)_3]$ by semi-preparative HPLC. The non-radioactive Re-DPA peptides were characterized by ESI-MS and MALDI-TOF-MS.

Labeling of DPA-peptides with [^{99m}Tc]Tc-tricarbonyl precursor

Two methods were used to label the DPA-conjugated peptides with ^{99m}Tc, in both cases the procedure required the use of an Isolink kit:

(1) One-pot method:

[^{99m}Tc]TcO_4^- eluate (800 µL, 600-800 MBq), DPA-conjugated peptide solution (20-40 µL: 20-40 µg DPA-peptide in H_2O) and MES buffer (200 µL, 1 M, pH 7.0) were mixed. Then the mixture was injected into the kit by a syringe. Subsequently, the mixture was heated at 95°C in oil bath for 30 min. Thereafter, the mixture was isolated by semi-preparative HPLC. The fraction of [^{99m}Tc]Tc-DPA-peptide was concentrated with a RP-18 cartridge and washed with ethanol/H_2O (2 mL, v/v: 1/1). Then ethanol was removed by N_2. The radiochemical purity of purified [^{99m}Tc]Tc-DPA-peptides was also monitored by semi-preparative HPLC.

(2) Two-pots method:

The first step was to prepare the [^{99m}Tc]Tc-tricarbonyl precursor by adding [^{99m}Tc]TcO_4^- into the Isolink kit. The second step was to coordinate the [^{99m}Tc]Tc-tricarbonyl moiety with a DPA-peptide.

Preparation of [^{99m}Tc]Tc-tricarbonyl precursor

[^{99m}Tc]TcO_4^- eluate (1.5 mL, 1-1.5 GBq) was added to Isolink kit. Subsequently, the glass vial was heated at 95°C in oil bath for 30 min; then cooling down the precursor. The radiochemical yield of the [^{99m}Tc]Tc-tricarbonyl precursor determined by ITLC (silica gel plate, mobile phase: CH_3OH/CH_2Cl_2, v:v: 1/5) and semi-preparative HPLC.

Preparation of [^{99m}Tc]Tc-DPA-peptides

MES buffer (500 µL, 1 M, pH 7.0) was added into [[^{99m}Tc]$Tc(OH_2)_3(CO)_3$] solution to adjust the pH to neutral. DPA-peptide solution (20-40 µL: 20-40 ug DPA-peptide in H_2O) was added into MES buffer (300 µL, 0.2 M, pH 6.2). Then [[^{99m}Tc]$Tc(H_2O)_3(CO)_3]^+$ solution (500 µL, 250-400 MBq) was added into the mixture. Subsequently, the mixture was kept in shaking stage for 60 min at 75°C.

Purification

Radiolabeled peptides were purified from the excess of reagent by semi-preparative HPLC. The fraction of [^{99m}Tc]-DPA-peptide was concentrated with a RP-18 cartridge and washed with water (10 mL) and eluted ethanol/H_2O (2 mL, v/v: 1/1). The loaded activity was collected. The solvent was removed by N_2. The radiochemical purity of purified [^{99m}Tc]Tc-DPA-peptide was monitored by semi-preparative HPLC.

Stability studies in buffer and human serum

[^{99m}Tc]Tc-**1**, [^{99m}Tc]Tc-**2** or [^{99m}Tc]Tc-**3** in high purity (each 100 µL) was added to PBS (pH 7.4) or human serum and incubated at 37°C. After 1 h and 24 h, the samples were withdrawn and analyzed by semi-preparative HPLC. To eliminate the protein fraction, the serum samples were first treated with ethanol (twice the volume) and centrifuged for 30 min at 4°C. The liquid phase was filtrated (VWR sterile syringe filter, 0.2 µm), and the filtrate was analyzed by semi-preparative HPLC to monitor the changes of the radiochemical purity.

Transchelation assays

[^{99m}Tc]Tc-**1**, [^{99m}Tc]Tc-**2** or [^{99m}Tc]Tc-**3** in high purity (each 100 µL) was added to propylene test tubes containing H_2O (50 µL), phosphate buffer (150 µL) and cysteine hydrochloride solution (100 µL, final: 10 mM or 1 mM) or histidine solution (100 µL, final: 10 mM or 1 mM). The mixture was vortexed and incubated at 37°C. At 1 h and 24 h aliquots of the reaction mixture were taken and analyzed by semi-preparative HPLC.

Determination of lipophilicity of ^{99m}Tc labeled peptides

[^{99m}Tc]Tc-**1**, [^{99m}Tc]Tc-**2** or [^{99m}Tc]Tc-**3** (each 50 µL, 0.2 MBq) was diluted in HEPES buffer (450 µL, 1 M, pH 7.4). *n*-Octanol (500 µL) was added and the mixture stirred vigorously for 30 min at 23°C. Subsequently, the mixture was centrifuged for 30 min (13.2 x 1000 *g*) at 23°C. Both water and n-octanol phases (450 µL), respectively, were taken and centrifuged again. The activity of both phases (each 100 µL) was measured in a gamma counter (Wallac 1480 Wizard 3" Automatic Gamma Counter, Perkin Elmer) and the octanol/water distribution coefficient (log $D_{o/w}$) was calculated with the equation as following: log $D_{o/w}$ = log [(Mean counts in octanol phase)/(Mean counts in water phase)]

Cell binding assays

Binding assays were assessed using cell homogenate of the murine melanoma cell line B16F10 (ATCC® CRL-6475™) as well as two human melanoma cell lines MeWo (ATCC® HTB-65™) and TXM13 (University of

Texas, M.D. Anderson Cancer Center, Houston, USA), and furthermore as MC1R-negative control the human embryonic kidney cell line HEK-293 (ATCC® CRL-1573™). The cells were grown as monolayer at 37°C in an incubator at CO_2/air (5%/95%) in DMEM medium with FCS (10%) (Biochrom AG). After washing the confluent cells twice with PBS and detaching them with trypsin/EDTA (0.05%/0.02%), the cells were suspended in DMEM (B16F10 about 1 Mio/mL; MeWo about 2 Mio/mL; TXM13 about 2 Mio/mL) and homogenized (Potter-Elvehjem) on ice. The assays were performed in a final volume of 200 µL.

Competition. In vitro binding affinity for non-radiolabeled peptides was assessed via competitive cell binding assays in B16F10 and MeWo cells using [^{125}I]I-NDP-MSH as standard radioligand. For one sample homogenized cells (156 µL) were incubated with [^{125}I]I-NDP-MSH (40 µL, final concentration 0.2 nM) in the presence of increasing of concentrations of **1**, **2**, **3** and Re-**1**, Re-**2**, Re-**3** (final concentrations 10^{-14} to 2.45×10^{-6} M for B16F10; 5.01×10^{-14} to 1.23×10^{-5} M for MeWo), as well as for comparison NDP-MSH (10^{-14} to 1.23×10^{-5} M) at 25°C for 90 min (n = 3).

Saturation. The binding affinities of the radiolabeled peptides ([^{99m}Tc]Tc-**1** or [^{99m}Tc]Tc-**2** or [^{99m}Tc]Tc-**3**) were determined in B16F10, MeWo, TXM13 and HEK293 cells. Homogenized cell suspension (158 µL) and cold PBS (2 µL) were added into a test tube for total binding evaluation (n = 3). Cells (158 µL) and NDP-MSH (2 µL, final 610 µM) were mixed into a test tube for unspecific binding evaluation (n = 2). Then, radiolabeled peptide (40 µL) with increasing concentrations (final 0.2-20 nM for [^{99m}Tc]Tc-**1** and [^{99m}Tc]Tc-**2** on B16F10 cells; 0.1-10 nM for [^{99m}Tc]Tc-**3** on B16F10 cells, 0.1-10 nM for [^{99m}Tc]Tc-**1** on both MeWo and TXM13 cells; 0.01-1 nM for [^{125}I]I-NDP-MSH on B16F10 and TXM13 cells; 0.02-2 nM for [^{125}I]I-NDP-MSH on MeWo cells) were added and incubated for 90 min at 25°C.

The incubation of all samples was stopped by washing the homogenate with cold PBS four times via a filter (Whatman GF/C, 90 min presoaked in 0.3% polyethyleneimine) using a cell harvester (Brandel, USA). The activity bound to the filter was measured in a gamma counter. In adjacent samples without cell homogenate the pure filter binding was determined. The experiments were performed three times. Pharmacological parameters such as inhibitory constant (K_i), dissociation constant (K_d) and maximal binding capacity (B_{max}) were calculated by fitting the data using a nonlinear curve fitting program (GraphPad Prism 5.02). Determination of protein content of the cell samples from the saturation assays was conducted with the bicinchoninic acid (BCA) protein assay kit (Pierce, Thermo Scientific) for calculation of B_{max} in fmol/mg protein.

Animal experiments

Animal experiments were performed in accordance to the guidelines of the German Regulations for Animal Welfare. The protocol was approved by the local Ethical Committee for Animal Experiments (reference number: 24-9168.21-4/2004-1). Healthy male Wistar rats (Wistar Unilever, HsdCpb: Wu, Harlan Winkelmann GmbH, Borchen, Germany) were housed under standard conditions with free access to standard food and tap water.

In vivo metabolite analysis. Rats (n = 4; body weight 180 ± 20 g) were anesthetized with desflurane (9 -10%, 30% oxygen/air). The threshold value for breathing frequency was 65 breaths/min. In supine position on a heating pad maintaining body temperature the rats were heparinized with 100 units/kg heparin (Heparin-Natrium 25.000-ratiopharm®, ratiopharm GmbH, Germany) by subcutaneous injection to prevent blood clotting on intravascular catheters. After local anesthesia with lignocaine (1%, Xylocitin®loc, mibe, Jena, Germany) into the right groin, a catheter (0.8 mm Umbilical Vessel Catheter, Tyco Healthcare, Tullamore, Ireland) was introduced into the right femoral artery for arterial blood sampling. A second needle catheter (35 G) was placed into a tail vein and used for [^{99m}Tc]Tc-**1** injection (15 MBq in 0.5 mL of infusions solution with 5% ethanol). Arterial blood samples were taken at 0, 5 and 60 min. Arterial plasma was separated by centrifugation (10 min at 1300 × *g*) followed by precipitation of the proteins with methanol (2 volumes of methanol to 1 volume of plasma) followed by 5 min storage at -60°C. A clear supernatant after centrifugation as well as urine samples (60 min p.i.) were used for metabolite analysis. For this the radio-HPLC system (Agilent 1100 series) was applied equipped with UV detection (254 nm) and an external radiochemical detector (Ramona, Raytest). Analysis was performed on a Zorbax C18 300SB (250 × 9.4 mm; 4 µm) column with an eluent system A (H_2O + 0.1% TFA) and B (CH_3CN + 0.1% TFA) in the following gradient: 0 - 30 min 95%-50% solvent A, flow rate, 3 mL/min.

Activity distribution in blood. To study activity distribution in blood, arterial blood samples were taken before (time point 0) and after injection of [^{99m}Tc]Tc-**1** at 2.5, 5, 10, 20, 30 and 60 min. Blood cells were separated by removing the clear supernatant after centrifugation (10 min at 1300 × *g*) of the blood samples at 4°C. The activity in blood cells and blood plasma was measured in a cross-calibrated well counter (WIZARD, Automatic Gamma Counter, Perkin Elmer, Waltham, MA, USA) or dose calibrator (Aktivimeter Isomed 2000; MED-Nuklear-Medizintechnik, Dresden, Germany).

In vivo biodistribution. For the biodistribution of [^{99m}Tc]Tc-**1**, two groups of rats (n = 8) were sacrificed under desflurane anesthesia at 5 and 60 min, respectively, after injection of [^{99m}Tc]Tc-**1** (500 µL, 0.30 ± 0.03 MBq). Organs and tissues of interest were removed, weighed, and the activity was measured in the cross-calibrated well counter or dose calibrator. The decay corrected data were normalized to the amount of injected activity calculated from the activity of injection syringes before and after injection and expressed as percentage of injected activity per gram tissue (%ID/g tissue) or standardized uptake values (SUV = ratio of activity per weight of tissue to injected activity per rat body weight). Values are quoted as mean ± standard deviation (mean ± SD) for one group of animals.

Acknowledgements

Feng Gao thanks the German Academic Exchange Service (DAAD) for financial support (A/11/94299, 91540213). The excellent technical assistance of Regina Herrlich, Utta Herzog and Andrea Suhr is greatly acknowledged.

Keywords: melanocortin-1 receptor • α-MSH analogs • peptides • [^{99m}Tc]Tc-tricarbonyl labeling • radiopharmaceuticals

References:

[1] a) S. M. Okarvi, *Med. research rev.* **2004**, *24*, 685-686; b) J. C. Reubi, *Endocr. Rev.* **2003**, *24*, 389-427; c) M. Fani, H. R. Maecke, S. M. Okarvi, *Theranostics* **2012**, *2*, 481-501.

[2] A. A. Rosenkranz, T. A. Slastnikova, M. O. Durymanov, A. S. Sobolev, *Biochemistry* **2013**, *78*, 1228-1237.

[3] N. Tandler, B. Mosch, J. Pietzsch, *Amino Acids* **2012**, *43*, 2203-2230.

[4] a) S. Froidevaux, M. Calame-Christe, J. Schuhmacher, H. Tanner, R. Saffrich, M. Henze, A. N. Eberle, *J. Nucl. Med.* **2004**, *45*, 116-123; b) Z. Cheng, Z. M. Xiong, M. Subbarayan, X. Y. Chen, S. S. Gambhir, *Bioconj. Chem.* **2007**, *18*, 765-772; c) J. P. Bapst, M. Calame, H. Tanner, A. N. Eberle, *Bioconj. Chem*. **2009**, *20*, 984-993; d) G. Nagy, N. Dénes, A. Kis, J. P. Szabó, E. Berényi, I. Garai, P. Bai, I. Hajdu, D. Szikra, G. Trencsényi, *Eur. J. Pharm. Sci.* **2017**, *106*, 336-344; e) F. Gao, W. Sihver, C. Jurischka, R. Bergmann, C. Haase-Kohn, B. Mosch, J. Steinbach, D. Carta, C. Bolzati, A. Calderan, J. Pietzsch, H. J. Pietzsch, *Amino Acids* **2016**, *48*, 833-847.

[5] a) A. Roxin, G. Zheng, *Future Med. Chem*. **2012**, *4*, 1601-1618; b) A. L. Tornesello, L. Buonaguro, M. L. Tornesello, F. M. Buonaguro, *Molecules* **2017**, *22*, pii: E1282.

[6] a) L. Wei, C. Butcher, Y. B. Miao, F. Gallazzi, T. P. Quinn, M. J. Welch, J. S. Lewis, *J. Nucl. Med.* **2007**, *48*, 64-72; b) M. V. Cantorias, S. D. Figueroa, T. P. Quinn, J. R. Lever,T. J. Hoffman, L. D. Watkinson, T. L. Carmack, C. S. Cutler, *Nucl. Med. Biol*. **2009**, *36*, 505-513; c) Z. Cheng, J. Chen, Y. Miao, N. K. Owen, T. P. Quinn, S. S. Jurisson, *J. Med. Chem.* **2002**, *45*, 3048-3056; d) Y. Miao, N. K. Owen, D. Whitener, F. Gallazzi, T. J. Hoffman, T. P. Quinn, *Int. J. Cancer* **2002**, 101, 480-487; e) P. McQuade, Y. Miao, J. Yoo, T. P. Quinn, M. J. Welch, J. S. Lewis, *J. Med. Chem*. **2005**, *48*, 2985-2992.

[7] a) A. P. Sattelberger, R. W. Atcher, *Nat. Biotechnol.* **1999**, *17*, 849-850; b) J. Fichna, A. Janecka, *Bioconj. Chem.* **2003**, *14*, 3-17.

[8] R. Alberto, *Eur. J.Inorg.Chem.* **2009**, *1*, 21-31.

[9] a) A. Stichelberger, R. Waibel, C. Dumas, P. A. Schubiger, R. Schibli, *Nucl. Med. Biol.* **2003**, *30*, 465-470; b) P. Kyprianidou, C. Tsoukalas, A. Chiotellis, D. Papagiannopoulou, C. P. Raptopoulou, A. Terzis, M. Pelecanou, M. Papadopoulos, I. Pirmettis, *Inorg. Chim. Acta* **2011**, *370*, 236-242.

[10] a) G. Gasser, A. M. Sosniak, A. Leonidova, H. Braband, N. Metzler-Nolte, *Aust. J. Chem.* **2011**, *64*, 265-272; b) L. Wyffels, B. D. Gray, C. Barber, J. M. Woolfenden, K. Y. Pak, Z. L. Liu, *Bioorgan. Med. Chem.* **2011**, *19*, 3425-3433.

[11] a) K. E. Bullok, M. Dyszlewski, J. L. Prior, C. M. Pica, V. Sharma, D. Piwnica-Worms, *Bioconj. Chem.* **2002**, *13*, 1226-1237; b) L. D. D'Andrea, I. Testa, M. Panico, R. Di Stasi, C. Caraco, L. Tarallo, C. Arra, A. Barbieri, A. Romanelli, L. Aloj, *Biopolymers* **2008**, *90*, 707-712.

[12] P. D. Raposinho, J. D. Correia, S. Alves, M. F. Botelho, A. C. Santos, I. Santos, *Nucl. Med. Biol*. **2008**,*35*, 91-99.

[13] M. Fani, H. R. Maecke, *Eur. J. Med. Mol. Imaging* **2012**, *39*, S11-S30.

[14] W. Siegrist, F. Solca, S. Stutz, L. Giuffre, S. Carrel, J. Girard, A. N. Eberle, *Cancer Res.* **1989**, *49*, 6352-6358.

[15] Y. B. Miao, D. Whitener, W. W. Feng, N. K. Owen, J. Q. Cheng, T. P. Quinn, *Bioconj. Chem.* **2003**, *14*, 1177-1184.

[16] R. Alberto, A. Egli, U. Abram, K. Hegetschweiler, V. Gramlich, P. A. Schubiger, *J. Chem. Soc. Dalton* **1994**, *19*, 2815-2820.

[17] D. D. Djokić, D. L. Janković, L. L. Stamenković, I. Pirmettis, *Nucl. Med. Rev. Cent. Eur.* **2004**, *7*, 1-5; G. E. Kodina, A. O. Malysheva, O. E. Klement'eva, A. A. Inkin, N. I. Gorshkov, A. A. Lumpov, D. N. Suglobov, *J. Nucl. Radiochem. Sci.* **2005**, *6*, 183-185.

[18] a) L. Radford, F. Gallazzi, L. Watkinson, T. Carmack, A. Berendzen, M. R. Lewis, S. S. Jurisson, D. Papagiannopoulou, H. M. Hennkens, *Nucl. Med. Biol.* **2017**, *47*, 4-9; b) R. Waibel, R. Alberto, J. Willuda, R. Finnern, R. Schibli, A. Stichelberger, A. Egli, U. Abram, J. P. Mach, A. Pluckthun, P. A. Schubiger, *Nat. Biotechnol.* **1999**, *17*, 897-901; c) R. Baishya, D. K. Nayak, S. Karmakar, S. Chattopadhyay, S. S. Sachdeva, B. R. Sarkar, S. Ganguly, M. C. Debnath, *Chem.Biol. Drug Des.* **2015**, *85*, 504-517; d) R. Schibli, P. A. Schubiger, *Eur. J. Nucl. Med. Mol. Imaging* **2002**, *29*, 1529-1542; e) L. O. T. Gainkam, L. Huang, V. Caveliers, M. Keyaerts, S. Hernot, I. Vaneycken, C. Vanhove, H. Revets, P. De Baetselier, T. Lahoutte, *J. Nucl. Med.* **2008**, *49*, 788-795[19] a) R. Misri, K. Saatchi, U. O. Hafeli, *Nucl. Med. Commun.* **2011**, *32*, 324-329; b) V. Akurathi, L. Dubois, N. G. Lieuwes, S. K. Chitneni, B. J. Cleynhens, D. Vullo, C. T. Supuran, A. M. Verbruggen, P. Lambin, G. M. Bormans, *Nucl. Med. Biol.* **2010**, *37*, 557-564; c) A. Ku, C. Chan, D. Scollard, R. Reilly, *J. Nucl. Med.* **2017**, *58*, (Suppl. 1), Abstract 673; d) C. J. Li, Y. X. Zhang, L. F. Wang, H. Y. Feng, X. T. Xia, J. Ma, H. Yuan, B. Gao, X. L. Lan, *Nucl. Med. Bio.* **2015**, *42*, 547-554; e) C. J. Li, B. Wen, L. F. Wang, H. Y. Feng, X. T. Xia, Z. L. Ding, B. Gao, Y. X. Zhang, X. L. Lan, *Nucl. Med. Commun.* **2015**, *36*, 452-460; f) S. Nawaz, G. E. D. Mullen, P. J. Blower, J. R. Ballinger, *Nucl. Med.Commun.* **2017**, *38*, 666-671; g) H. Carpenet, A. Cuvillier, J. Monteil, I. Quelven, *Plos One* **2015**, *10*, e0139835.

[20] D. Carta, N. Salvarese, N. Morellato, F. Gao, W. Sihver, H. J. Pietzsch, B. Biondi, P. Ruzza, F. Refosco, D. Carpanese, A. Rosato, C. Bolzati, *Nucl. Med. Biol*. **2016**, *43*, 788-801.

[21] H. M. Bigott-Hennkens, S. F. Dannoon, S. M. Noll, V. C. Ruthengael, S. S. Jurisson, M. R. Lewis, *Nucl. Med.Biol.* **2011**, *38*, 549-555.

[22] a) G. R. Morais, A. Paulo, I. Santos, *Organometallics* **2012**, *31*, 5693-5714; b) G. Z. Liu, S. P. Dou, J. He, J. L. Vanderheyden, M. Rusckowski, D. J. Hnatowich, *Bioconj. Chem.* **2004**, *15*, 1441-1446; d) T. Storr, Y. Sugai, C. A. Barta, Y. Mikata, M. J. Adam, S. Yano, C. Orvig, *Inorg. Chem.* **2005**, *44*, 2698-2705.

[23] a) D. Shamshirian, M. Erfani, D. Beiki, M. Hajiramazanali, B. Fallahi, *Iran J. Pharm. Res.* **2016**, *15*, 349-360; c) M. F. Garcia, X. L. Zhang, F. Gallazzi, M. Fernandez, M. Moreno, J. P. Gambini, W. Porcal, P. Cabral, T. P. Quinn, *Anticancer Agents Med. Chem.* **2015**, *15*, 122-130.

[24] P. A. Rasposinho, C. Xavier, J. D. Correia, S. Falcão, P. Gomes, I. Santos, J. Biol. Inorg. Chem. 2008, 13, 449-459.

[25] a) W. Siegrist, A. N. Eberle, *Trends Endocrin. Met.* **1995**, *6*, 115-120; b) B. Loir, C. P. Sanchez, G. Ghanem, J. A. Lozano, J. C. Garcia-Borron, C. Jimenez-Cervantes, *Cell. Mol. Biol.***1999**, *45*, 1083-1092.

[26] a) H. B. Schioth, V. Chhajlani, R. Muceniece, V. Klusa, J. E. S. Wikberg, *Life Sci.* **1996**, *59*, 797-801; b) J. Chluba-de Tapia, C. Bagutti, R. Cotti, A. N. Eberle, *J. Cell Sci.* **1996**, *109*, 2023-2030.

[27] a) W. Siegrist, M. Oestreicher, S. Stutz, J. Girard, A. N. Eberle, *J. Receptor Res.***1988**, *8*, 323-343; b) W. Siegrist, D. H. Willard, W. O.Wilkison, A. N. Eberle, *Biochem. Bioph. Res. Commun.* **1996**, *218*, 171-175; c) A. N. Eberle, V. J. Verin, F. Solca, W. Siegrist, C. Kuenlin, C. Bagutti, S. Stutz, J. Girard, *J. Receptor Res.* **1991**, *11*, 311-322; d) J. Lunec, C. Pieron, A. J. Thody, *Melanoma Res.* **1992**, *2*, 5-12; e) H. B. Schioth, P. Yook, R. Muceniece, J. E. S. Wikberg, M. Szardenings, *Mol. Pharmacol.* **1998**, *54*, 154-161; f) A. Ringholm, J. Klovins, R. Rudzish, S. Phillips, J. L. Rees, H. B. Schioth, *J. Invest. Dermatol.* **2004**, *123*, 917-923.

[28] R. D. Cone, K. G. Mountjoy, L. S. Robbins , J. H. Nadeau, K. R. Johnson, L. Roselli-Rehfuss, M. T. Mortrud, *Ann. N. Y. Acad. Sci.* **1993**, *680*, 342-363.

[29] J. Q. Chen, Z. Cheng, T. J. Hoffman, S. S. Jurisson, T. P. Quinn, *Cancer Res.* **2000**, *60*, 5649-5658.

[30] S. Froidevaux, M. Calame-Christe, H. Tanner, A. N. Eberle, *J. Nucl. Med.* **2005**, *46*, 887-895.

[31] a) Z. Cheng, J. Q. Chen, T. P. Quinn, S. S. Jurisson, *Cancer Res.* **2004**, *64*, 1411-1418; b) M. F. Giblin, N. Wang, T. J. Hoffman, S. S. Jurisson, T. P. Quinn, *Proc. Natl. Acad. Sci. USA* **1998**, *95*, 12814-12818.

[32] H. Guo, Y. Miao, *Mol. Pharmaceutics* **2012**, *9*, 2322-2330; J. C. Lim, Y. D. Hong, J. J. Kim, S. M. Choi, H. S. Baek, S. J. Choi, *Cancer Biother. Radiopharm.* **2012**, *27*, 464-472.

[33] M. Morais, B. L. Oliveira, J. D. G. Correia, M. C. Oliveira, M. A. Jimenez, I. Santos, P. D. Raposinho, *J. Med. Chem.* **2013**, *56*, 1961-1973.

[34] Y. Funasaka, H. Sato, A. K. Chakraborty, A. Ohashi, G. P. Chrousos, M. Ichihashi, *J. Investig. Dermatol. Symp. Proc.* **1999**, *4*, 105-109.

[35] G. Petrangolini, G. Pratesi, M. De Cesare, R. Supino, C. Pisano, M. Marcellini, V. Giordano, D. Laccabue, C. Lanzi, F. Zunino, *Mol. Cancer Res.* **2003**, *1*, 863-870.

[36] B. Holst, C. E. Elling, T. W. Schwartz, *J. Biol. Chem.* **2002**, *277*, 47662-47670.

[37] T. K. Sawyer, P. J. Sanfilippo, V. J. Hruby, M. H. Engel, C. B. Heward, J. B. Burnett, M. E. Hadley, *Proc Natl Acad Sci U S A*. **1980**, *77*, 5754-5758.

[38] a) M. Gotthardt, J. van Eerd-Vismale, W. J. Oyen, M. de Jong, H. Zhang, E. Rolleman, H. R. Maecke, M. Behe, O. Boerman, *J. Nucl. Med*. **2007**, *48*, 596-601; b) J. Yang, J. Lu, Y. Miao, *Mol. Pharm*. **2012**, *9*, 1418-1424; c) J. B. Bapst, A. N. Eberle, *Front. Endocrinol*. **2017**, *8*, 93.

[39] a) E. I. Christensen, H. G. Rennke, F. A. Carone, *Renal. Physiol.* **1983**, *244*, F436–F441; b) E. G. Garayoa,C. Schweinsberg, V., L. Brans, P. Bläuenstein, D. A. Tourwé, R. Schibli, P. A. Schubiger, *Bioconj. Chem.* **2008,** *19,* 2409–2416;c) H. Akizawa, Y. Arano, M. Mifune, A. Iwado, Y. Saito, T. Mukai, T. Uehara, M. Ono, Y. Fujioka, K. Ogawa, Y. Kiso, H. Saji, *Nucl. Med. Biol.* **2001**, *28*, 761-768.

[40] T. M. Behr, D. M. Goldenberg, W. Becker, *Eur. J.Nucl. Med.* **1998**, *25*, 201-212.

[41] T. Maack, V. Johnson, S. T. Kau, J. Figueiredo, D. Sigulem, *Kidney Int.* **1979**, *16*, 251-270.

[42] A. M. Flook, J. Q. Yang, Y. B. Miao, *Mol. Pharm.* **2013**, *10*, 3417-3424.

[43] B. B. Kasten,X. Ma, H. Liu, T. R. Hayes, C. L. Barnes, S. Qi, K. Cheng, S. C. Bottorff, W. S. Slocumb, J. Wang, Z. Cheng, P. D. Benny, Bioconjug. Chem. 2014, 25, 579-592.

[44] a) J. M. Heldt, O. Kerzendorfer, C. Mamat, F. Starke, H. J. Pietzsch, J. Steinbach, *Synlett* **2013**, *24*, 432-436; b) H. Stephan, M. Walther, S. Fähnemann, P. Ceroni, J. K. Molloy, G. Bergamini, F. Heisig, C. E. Muller, W. Kraus, P. Comba, *Chem.-Eur. J.* **2014**, *20*, 17011-1701